Supplementary materials

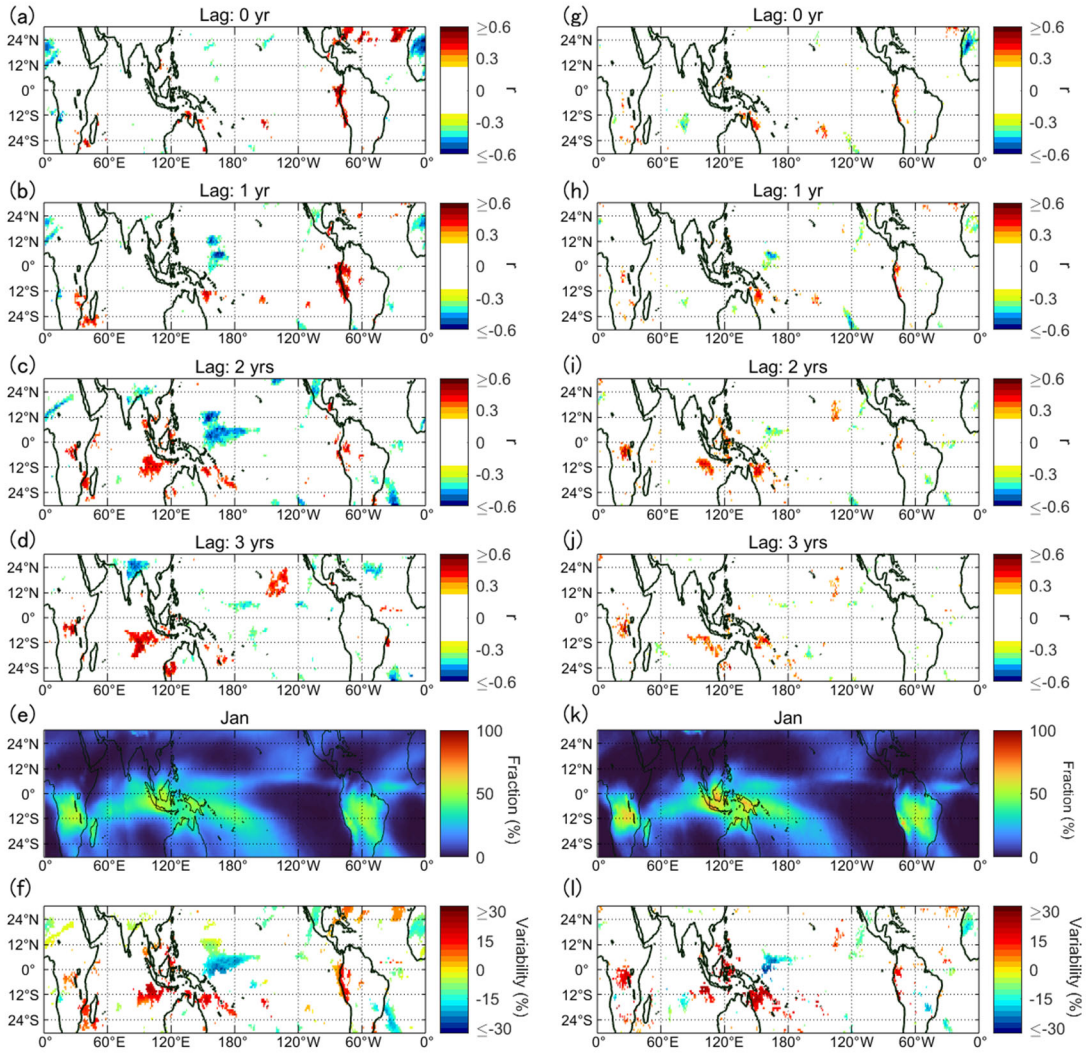

Figure S1. (a-d) Correlation coefficient r ($p \leq 0.05$) between GCRs and the high-altitude cloud fraction in January by ISCCP for a time lag of 0–3years, respectively. (e) Monthly mean fraction of the high-altitude clouds in January. (f) Maximal variability of the high-altitude cloud fraction over the GCR cycles. (g-l) Same as (a-f) but for the high-altitude clouds, as monitored using OLR.

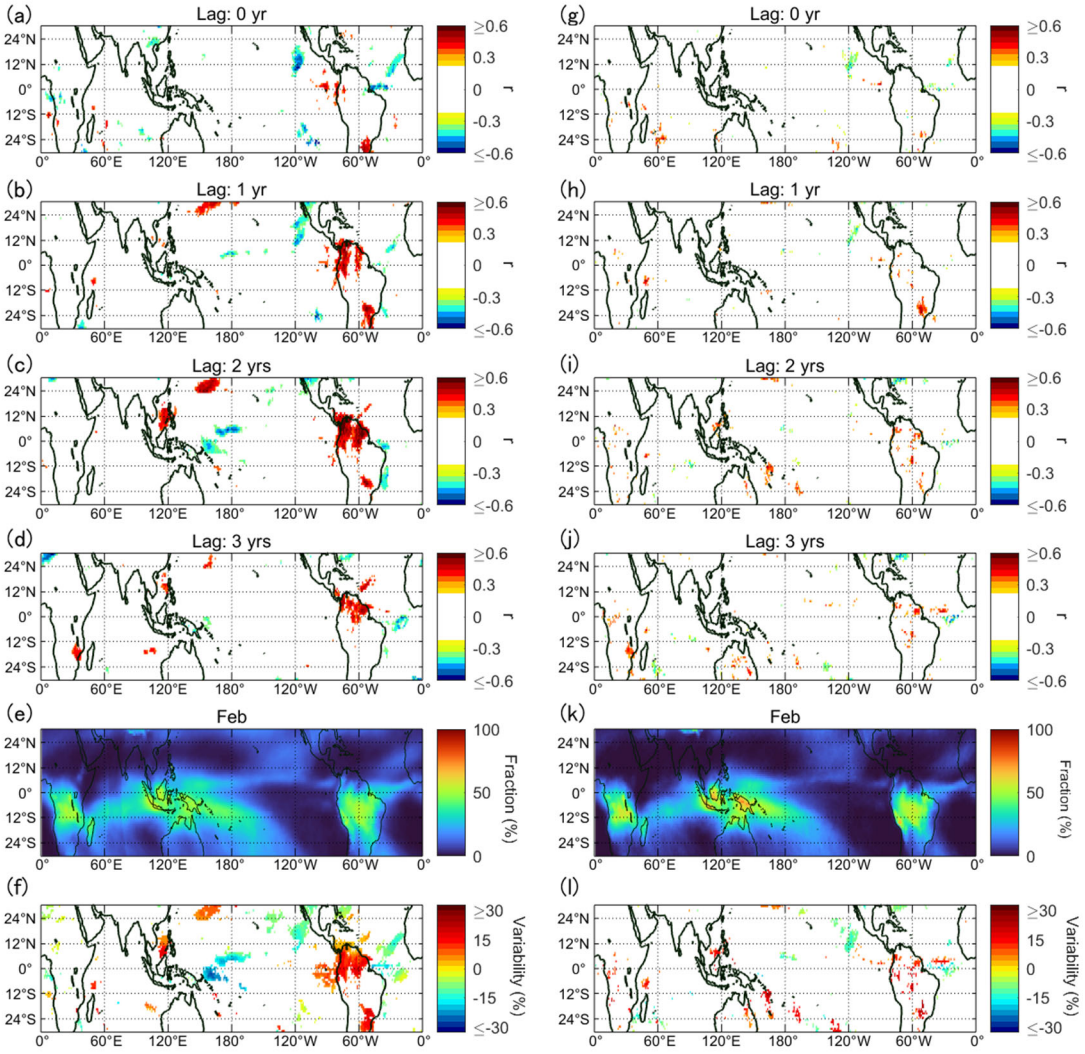

Figure S2. Same as Fig. S1 but for February.

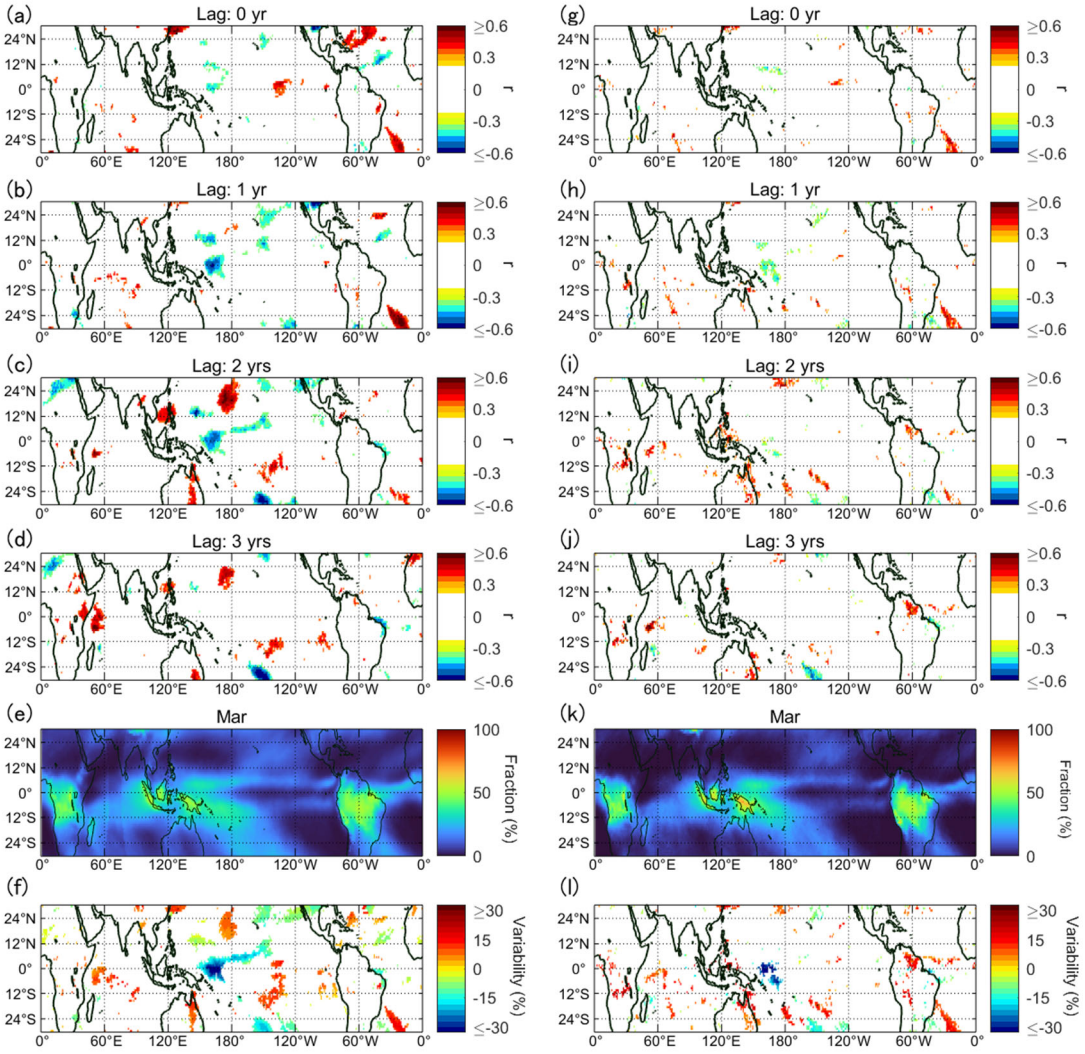

Figure S3. Same as Fig. S1 but for March.

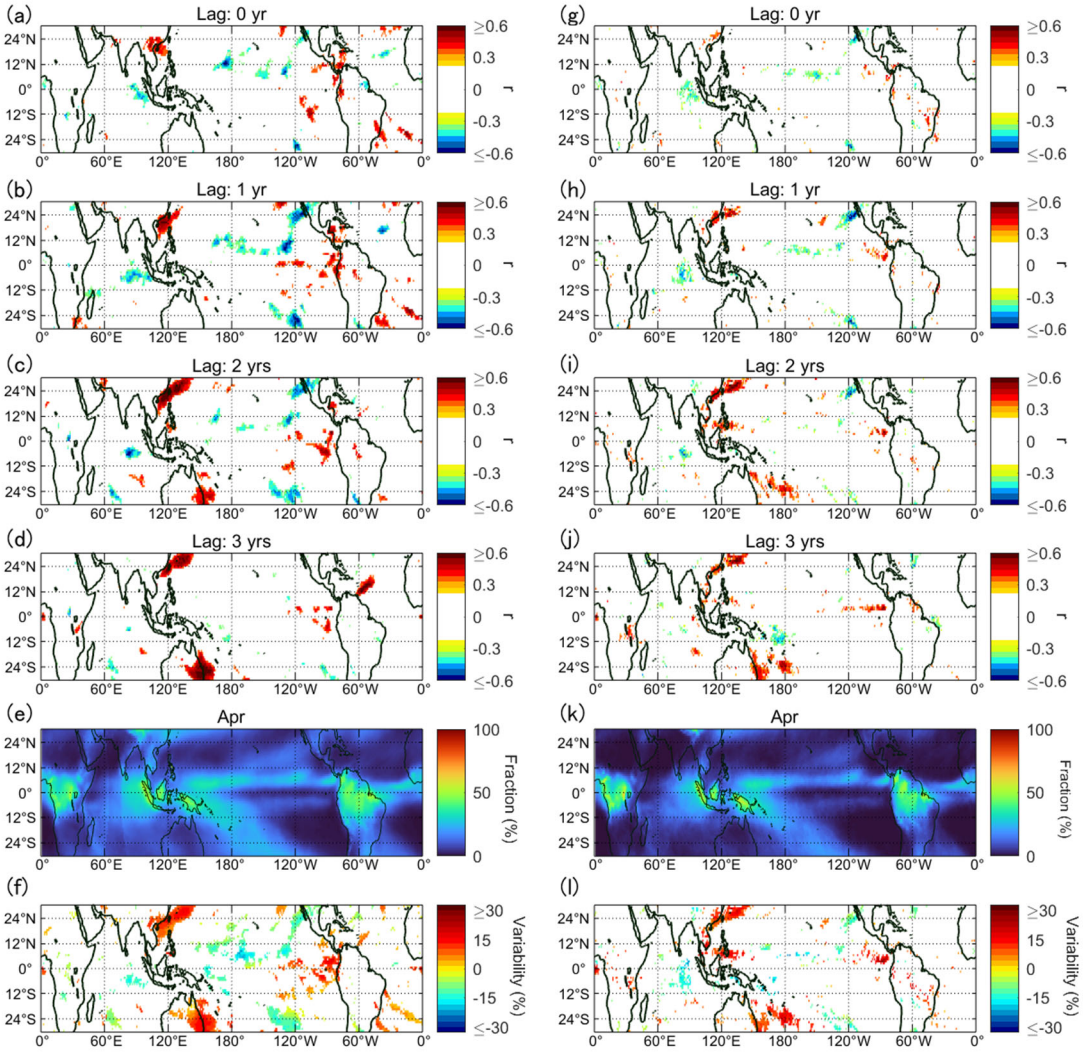

Figure S4. Same as Fig. S1 but for April.

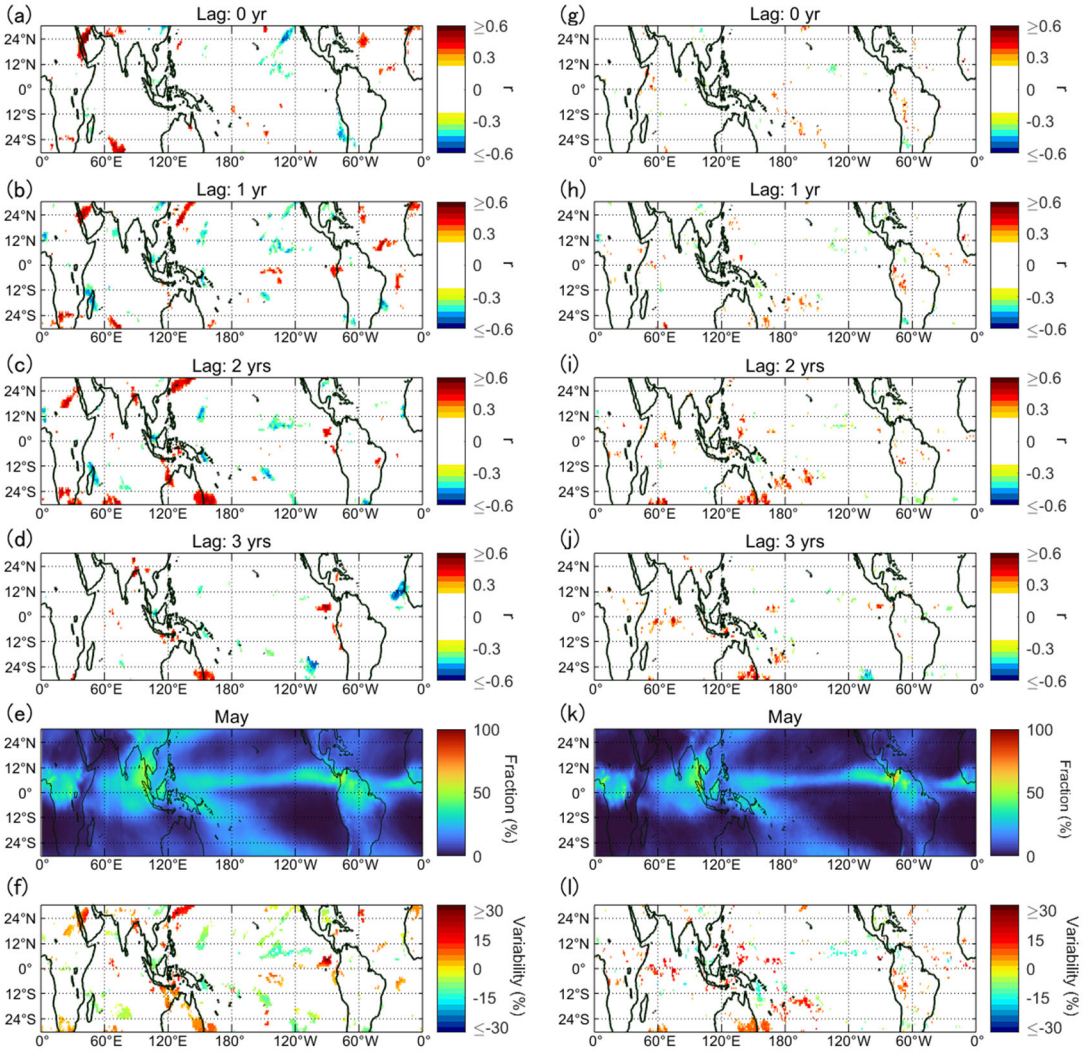

Figure S5. Same as Fig. S1 but for May.

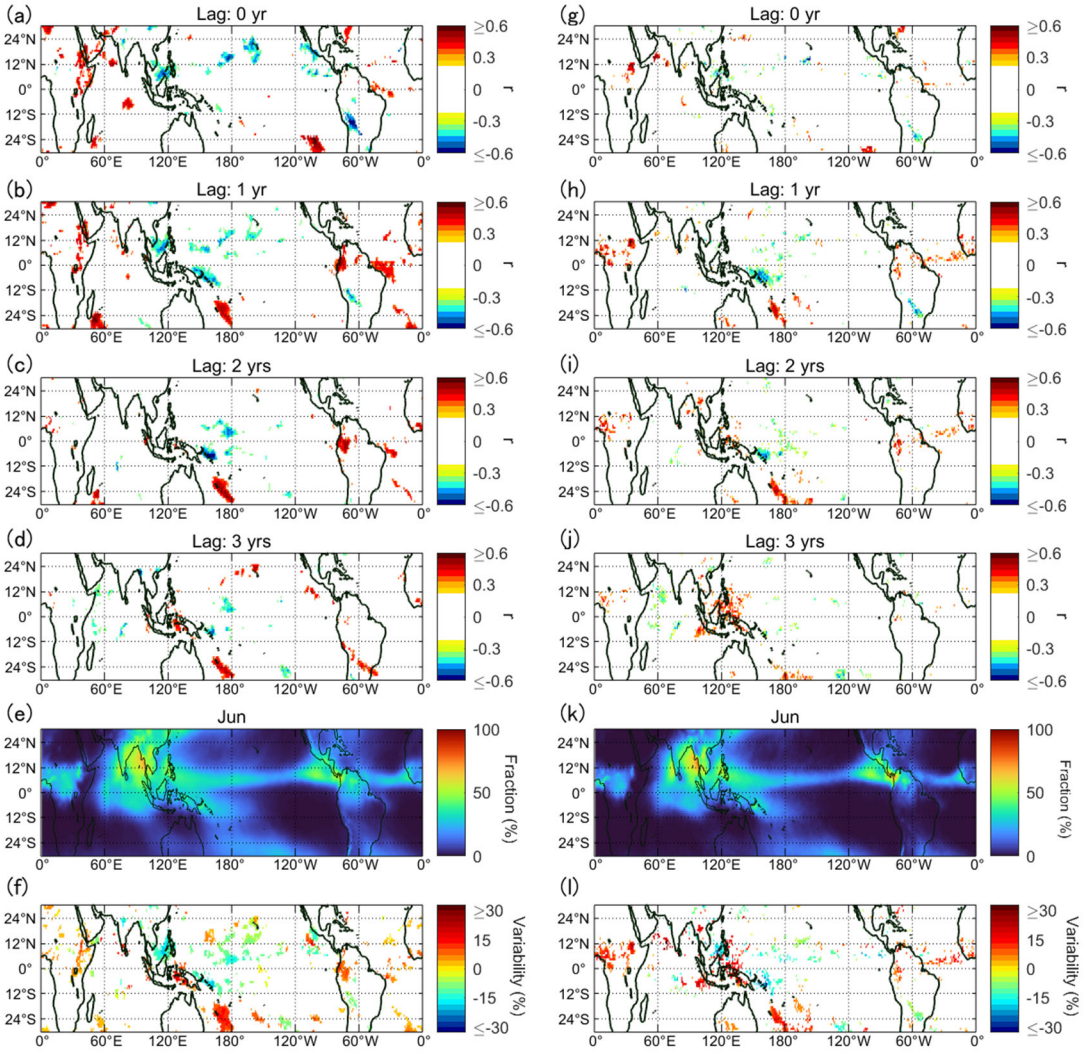

Figure S6. Same as Fig. S1 but for June.

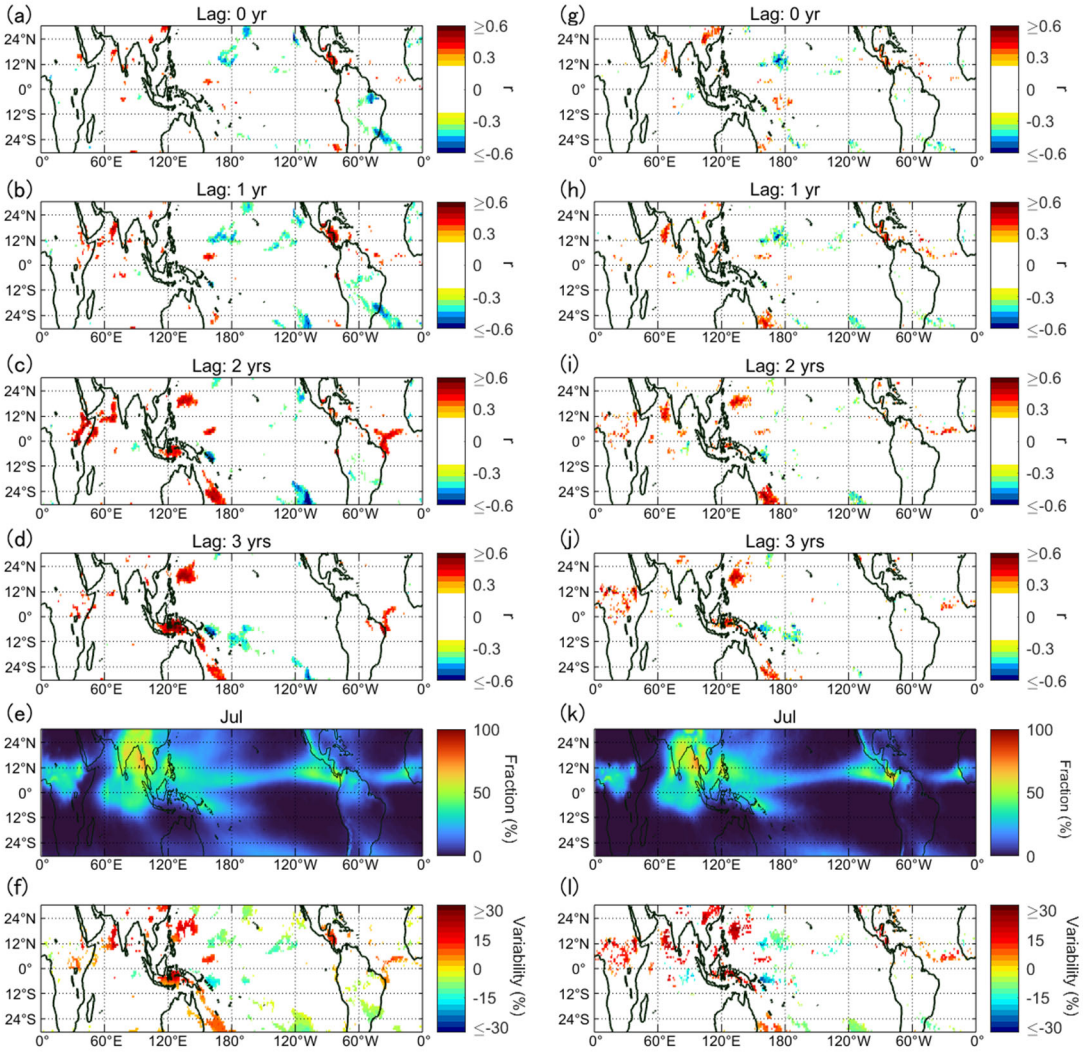

Figure S7. Same as Fig. S1 but for July.

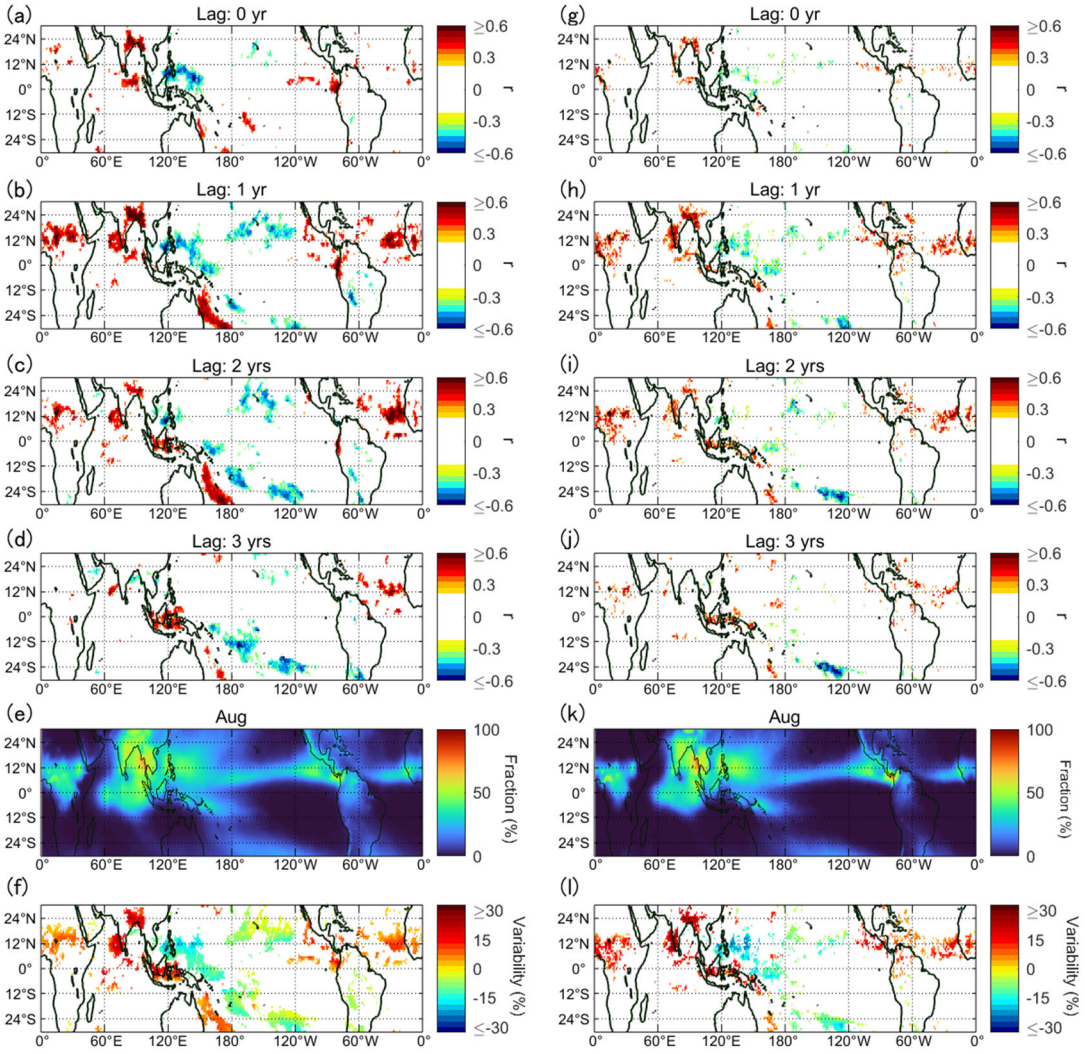

Figure S8. Same as Fig. S1 but for August.

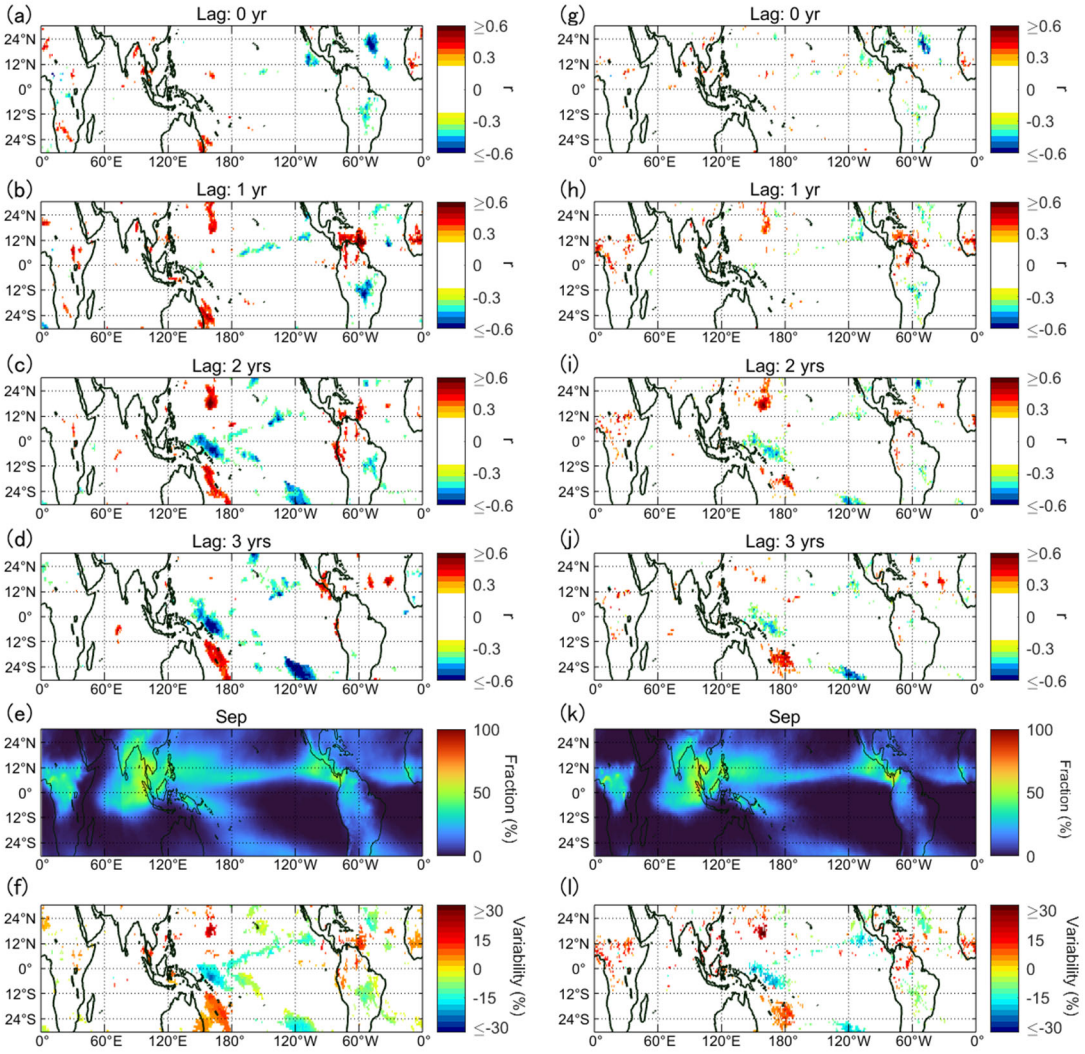

Figure S9. Same as Fig. S1 but for September.

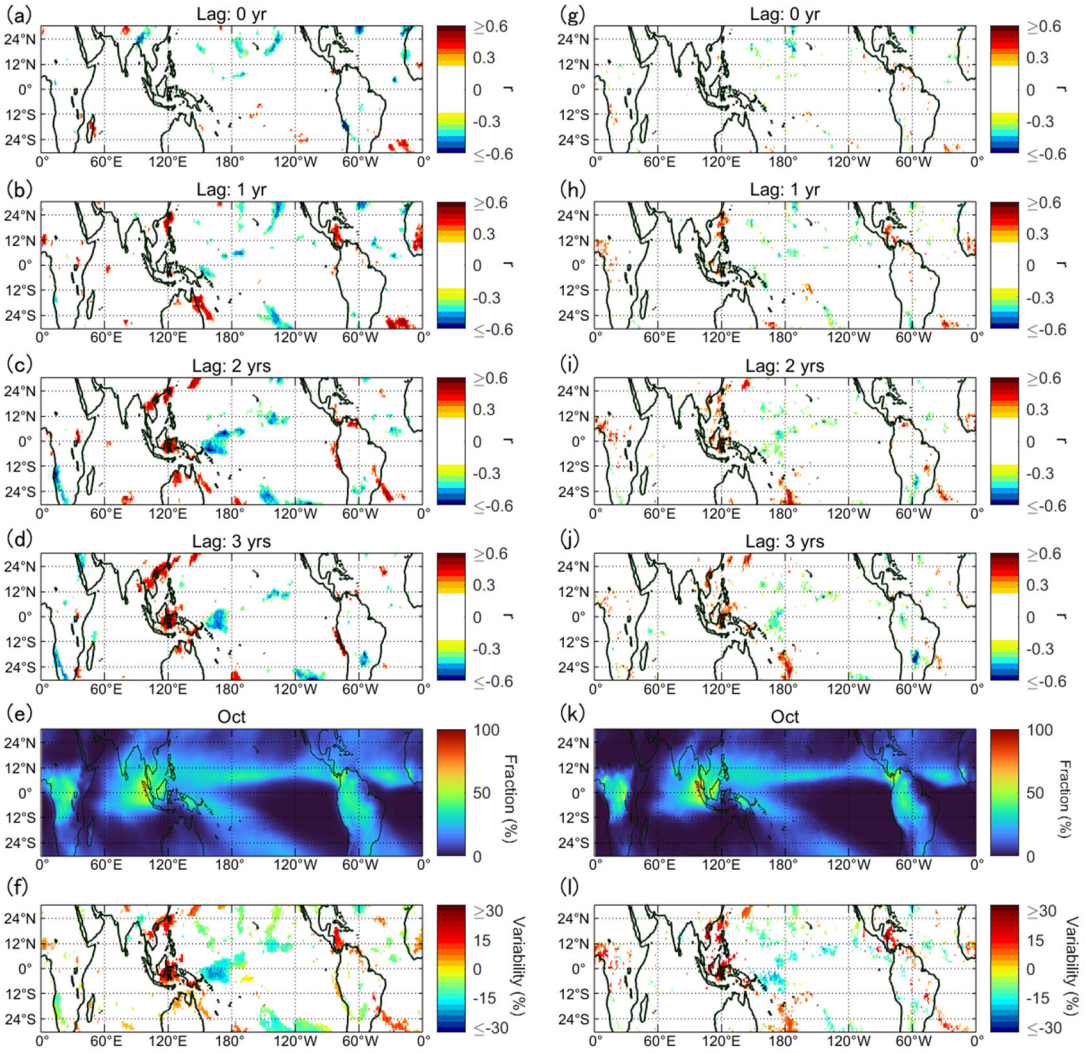

Figure S10. Same as Fig. S1 but for October.

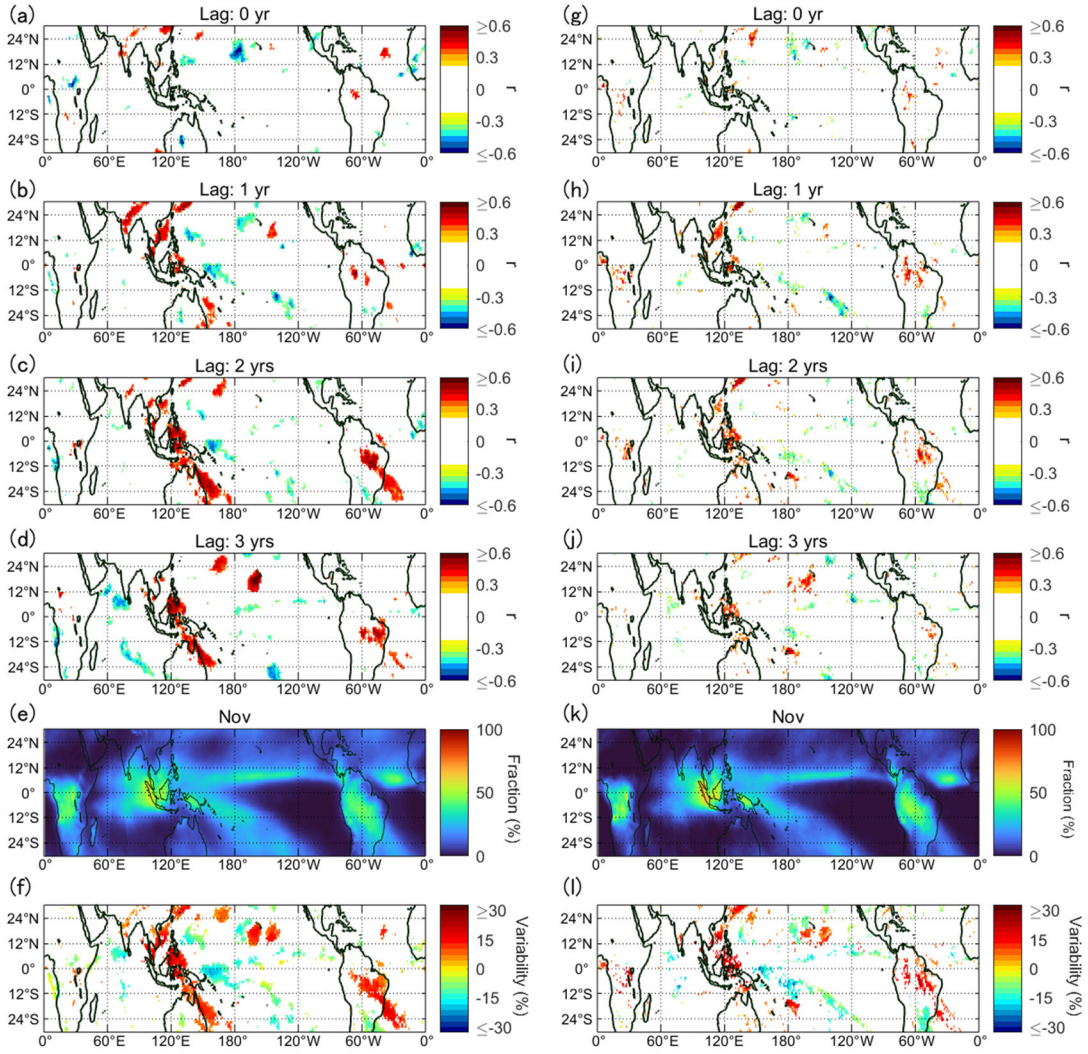

Figure S11. Same as Fig. S1 but for November.

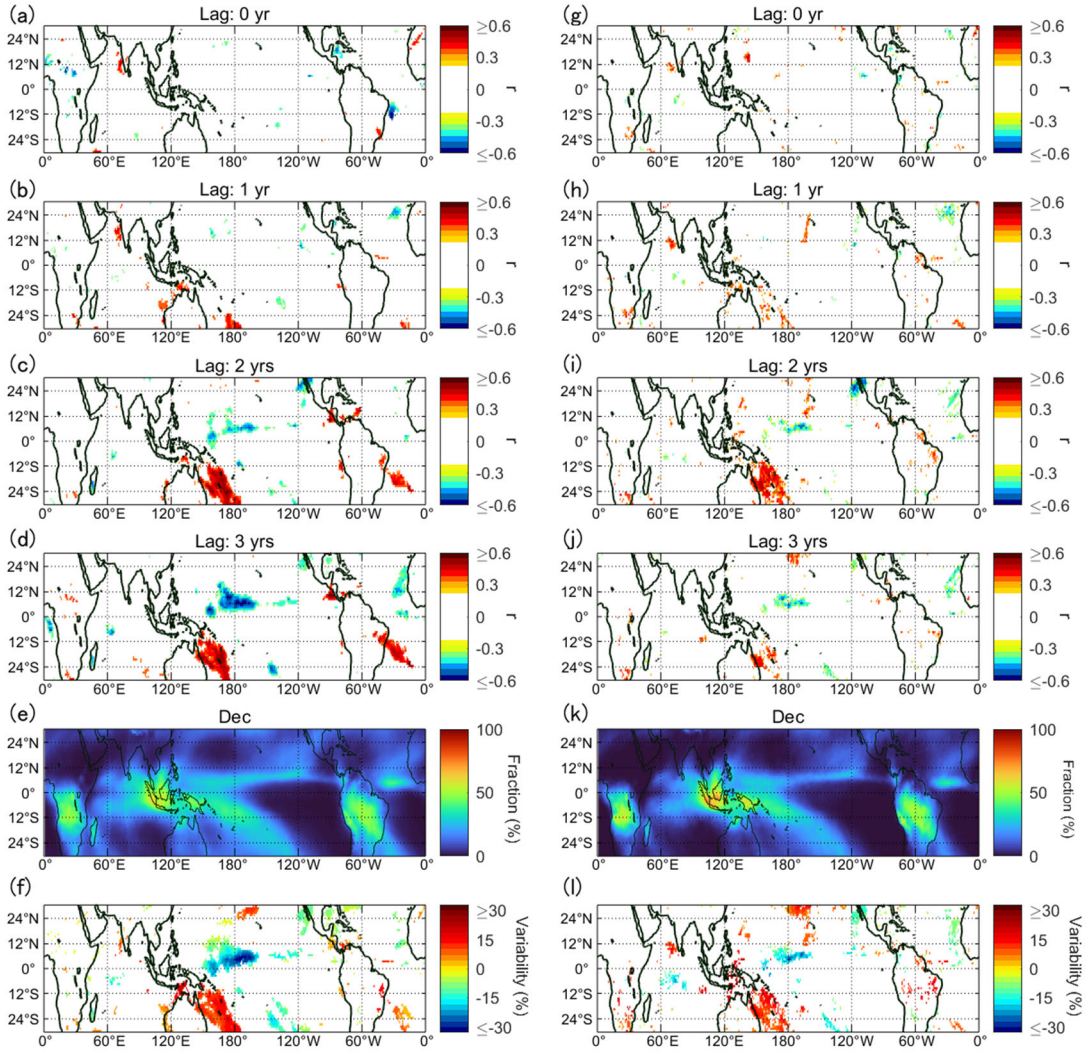

Figure S12. Same as Fig. S1 but for December.

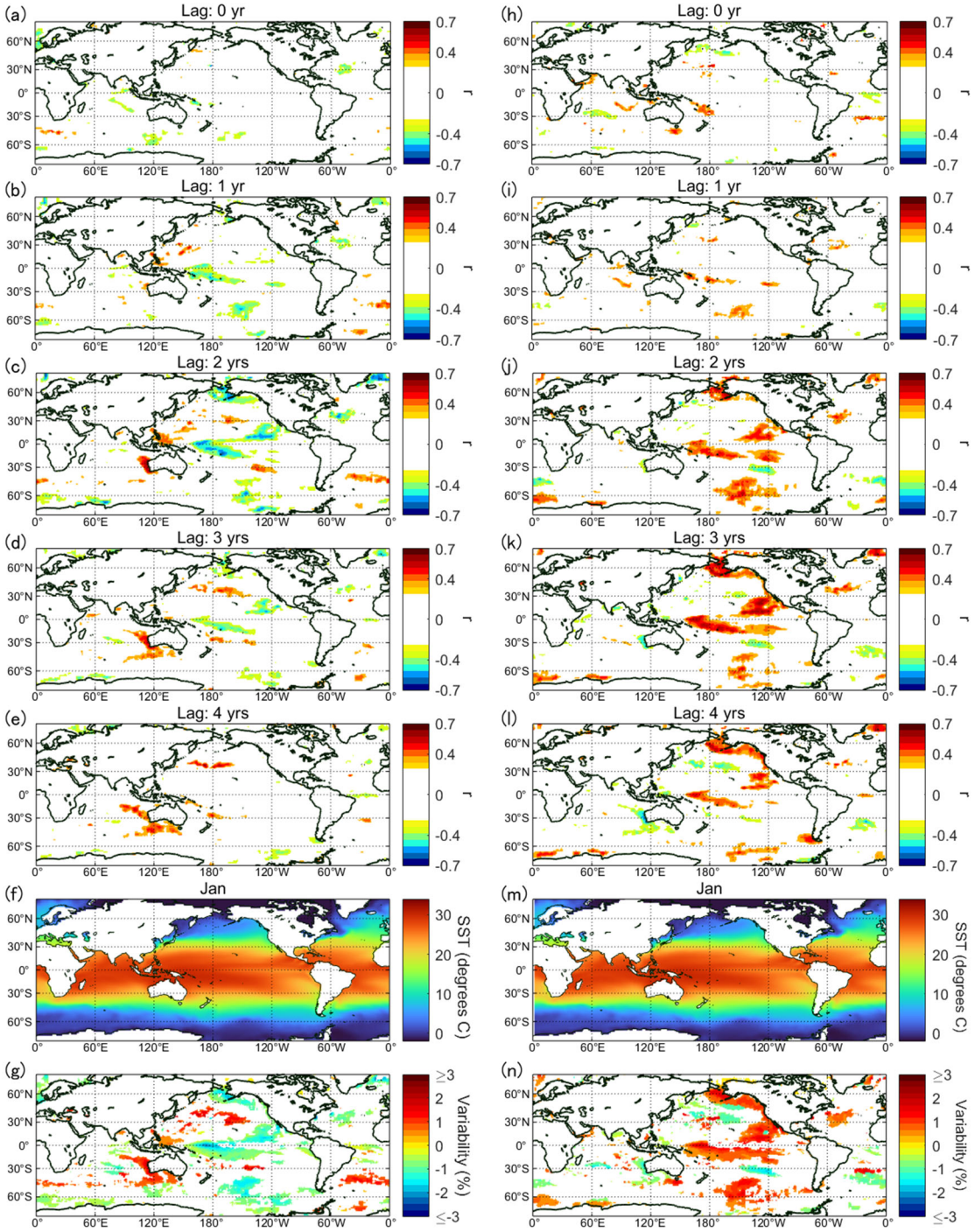

Figure S13. (a-e) Correlation coefficient r ($p \leq 0.05$) between GCR and SST in January for a time lag of 0–4years, respectively. (f) Monthly mean SST. (g) Maximal variability of SST over the GCR cycles. (h-n) Same as (a-g) but for TSI.

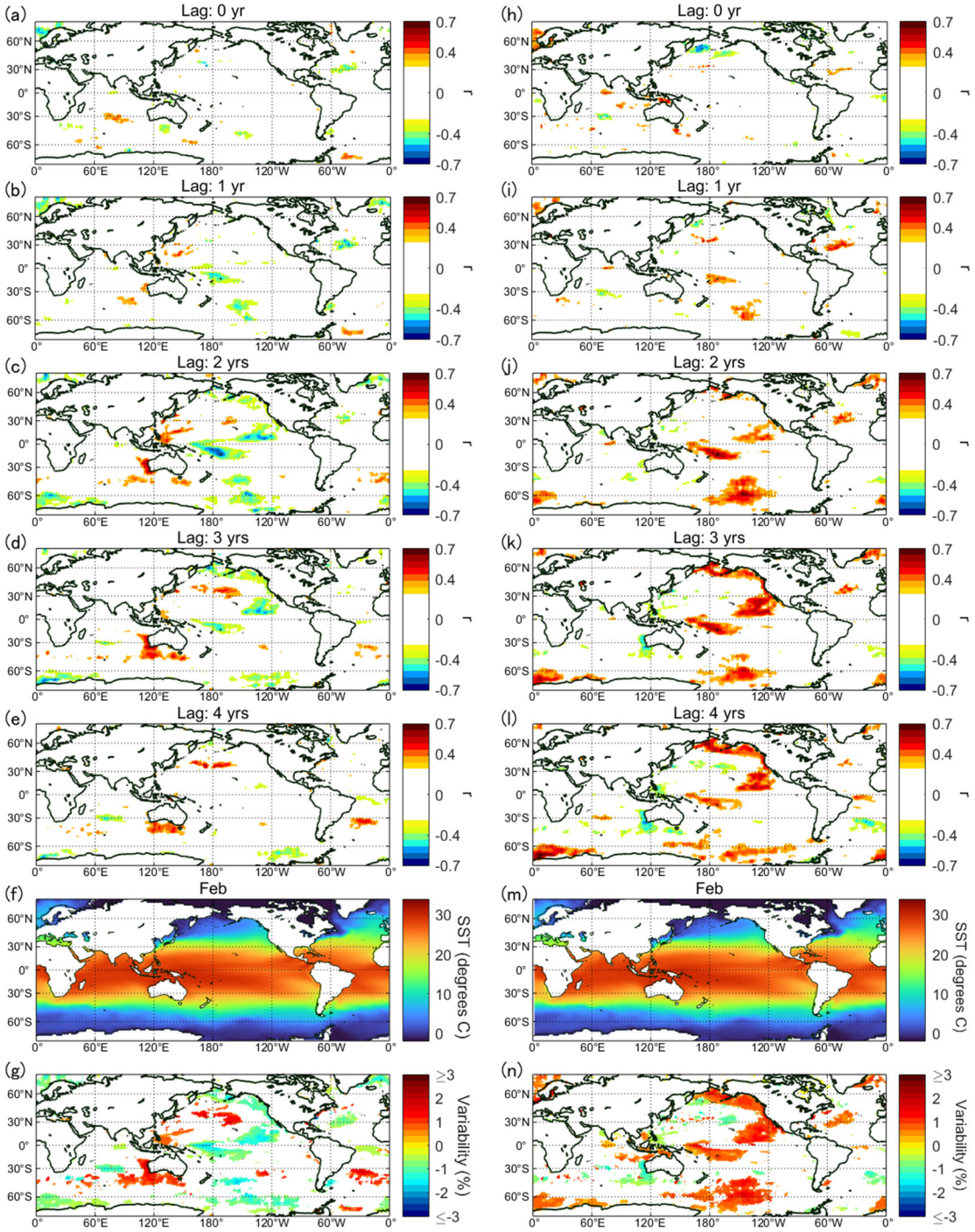

Figure S14. Same as Fig. S13 but for February.

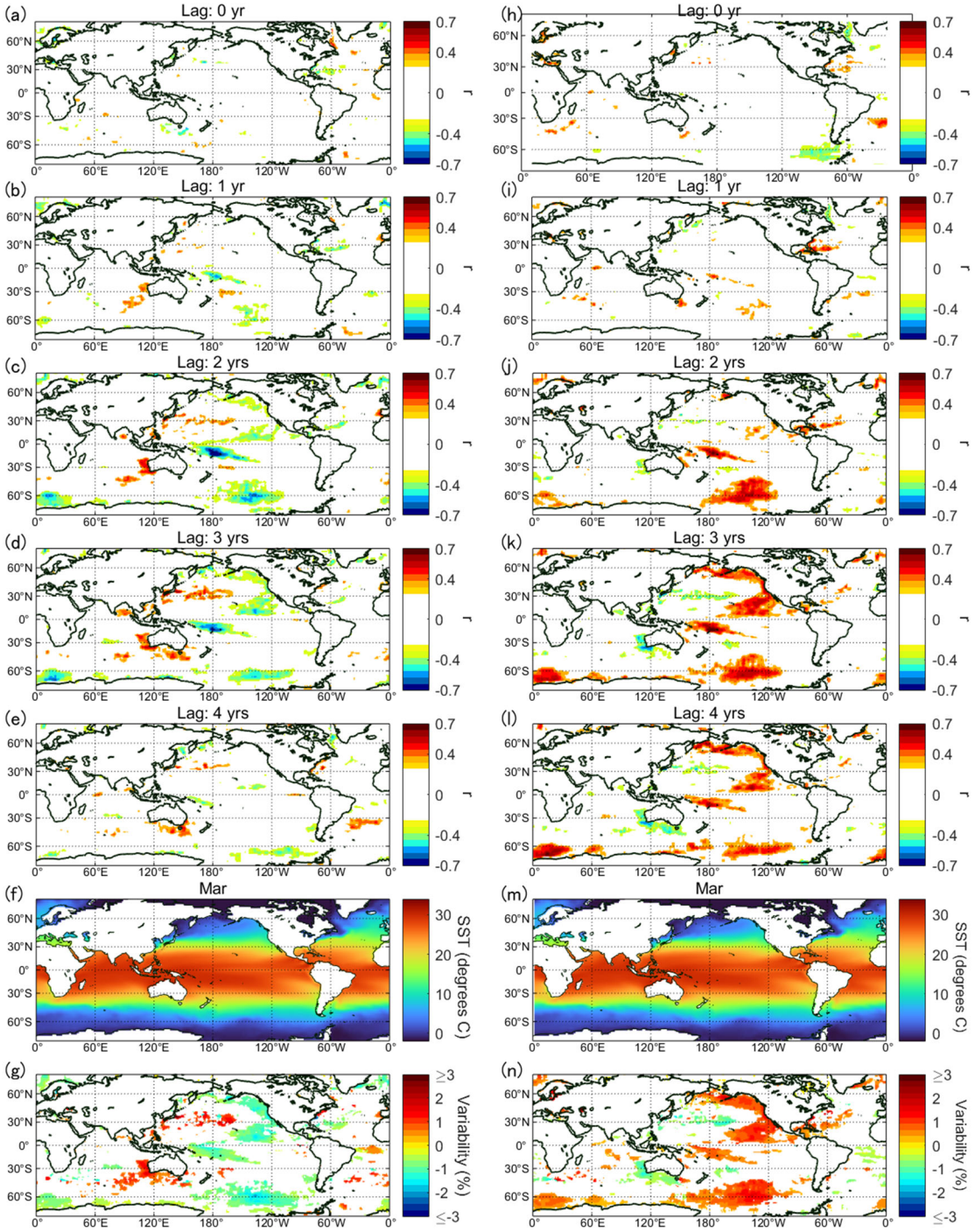

Figure S15. Same as Fig. S13 but for March.

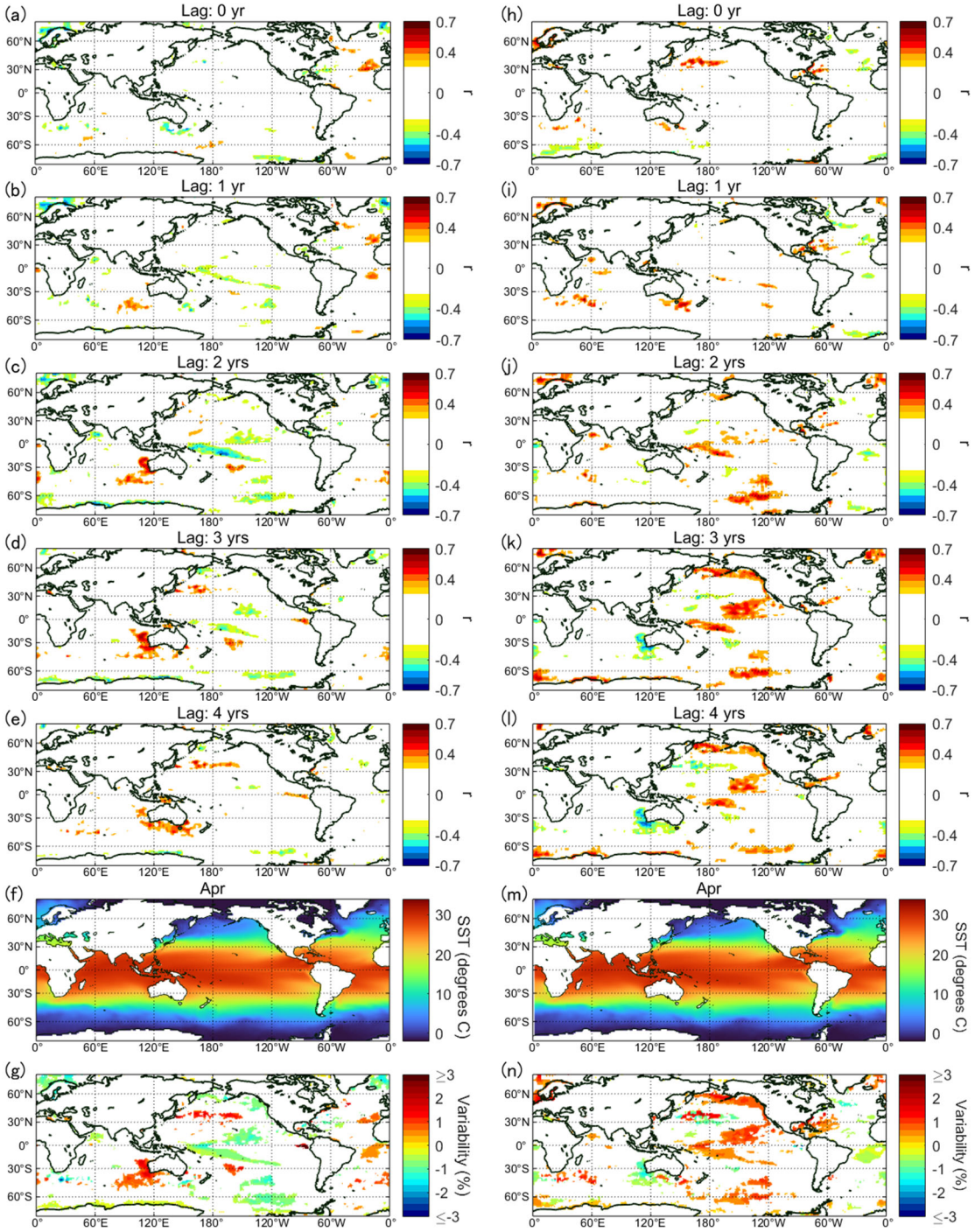

Figure S16. Same as Fig. S13 but for April.

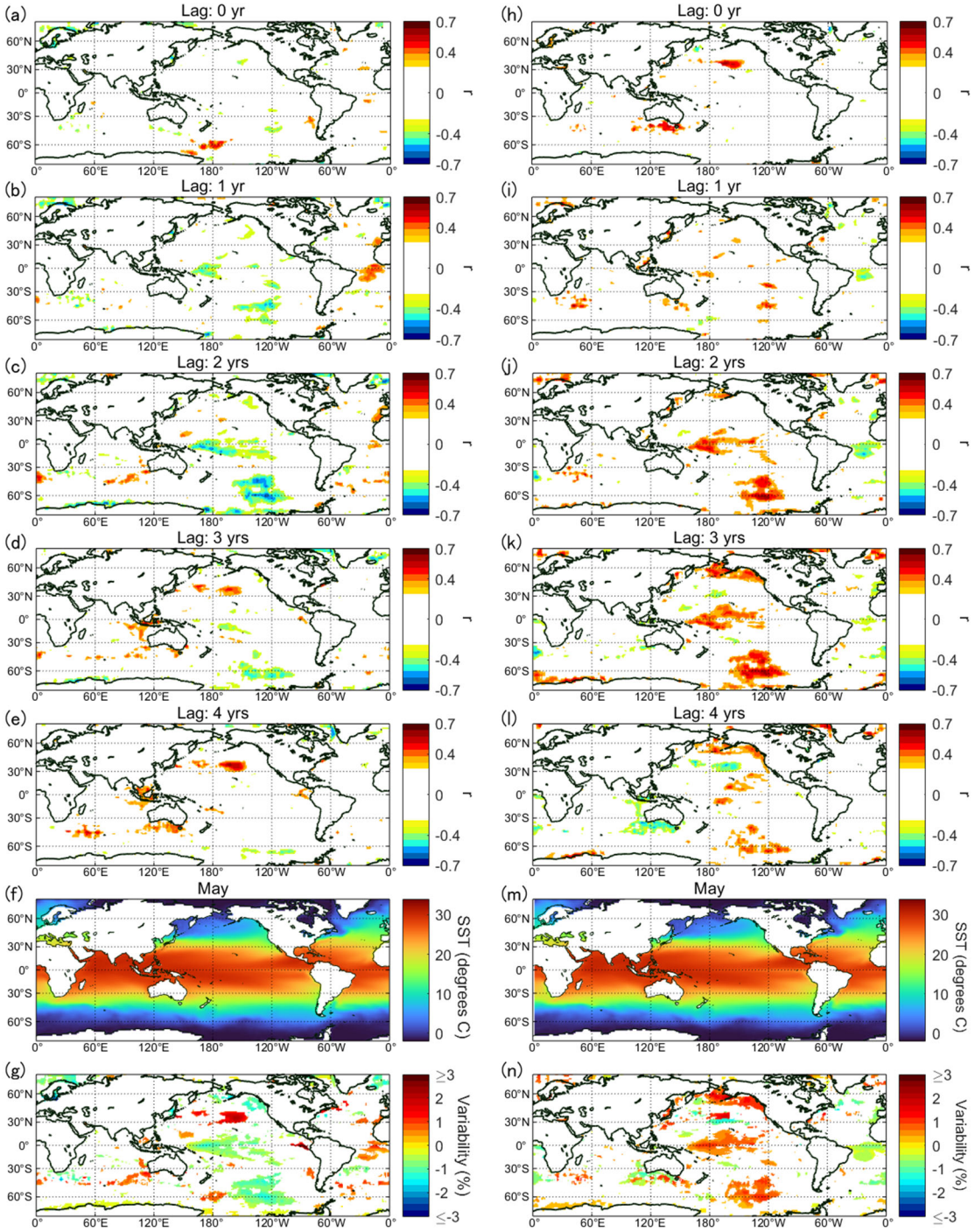

Figure S17. Same as Fig. S13 but for May.

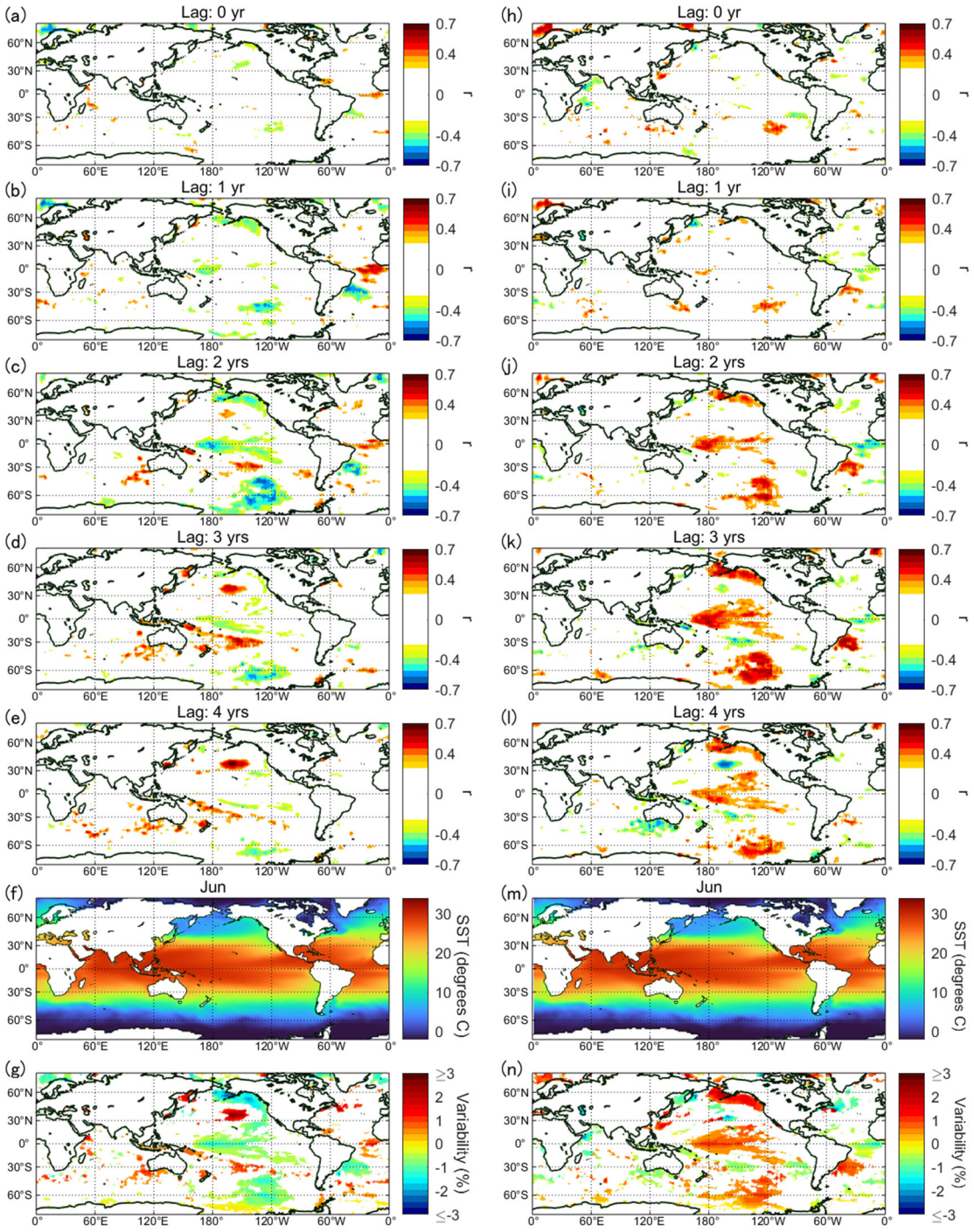

Figure S18. Same as Fig. S13 but for June.

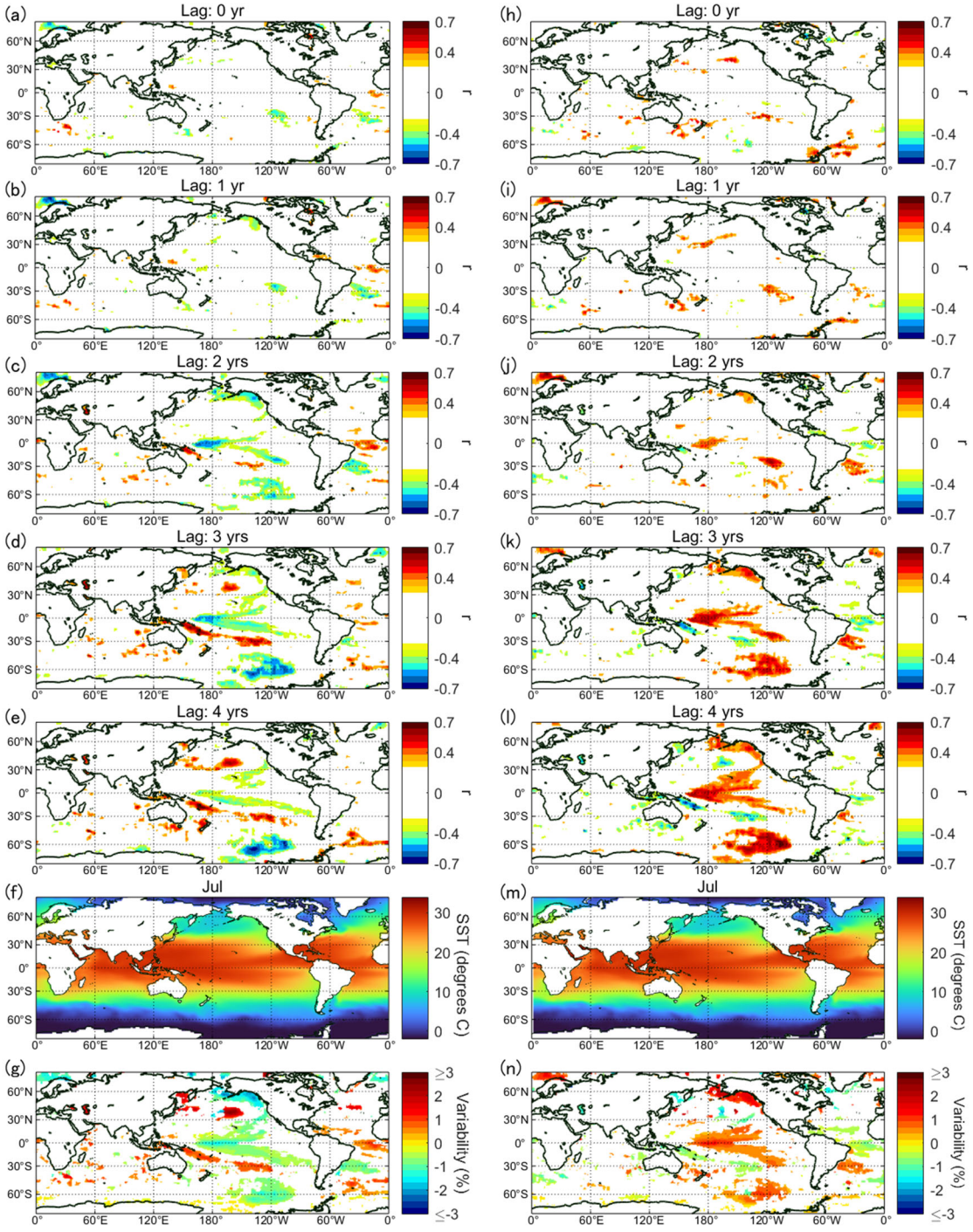

Figure S19. Same as Fig. S13 but for July.

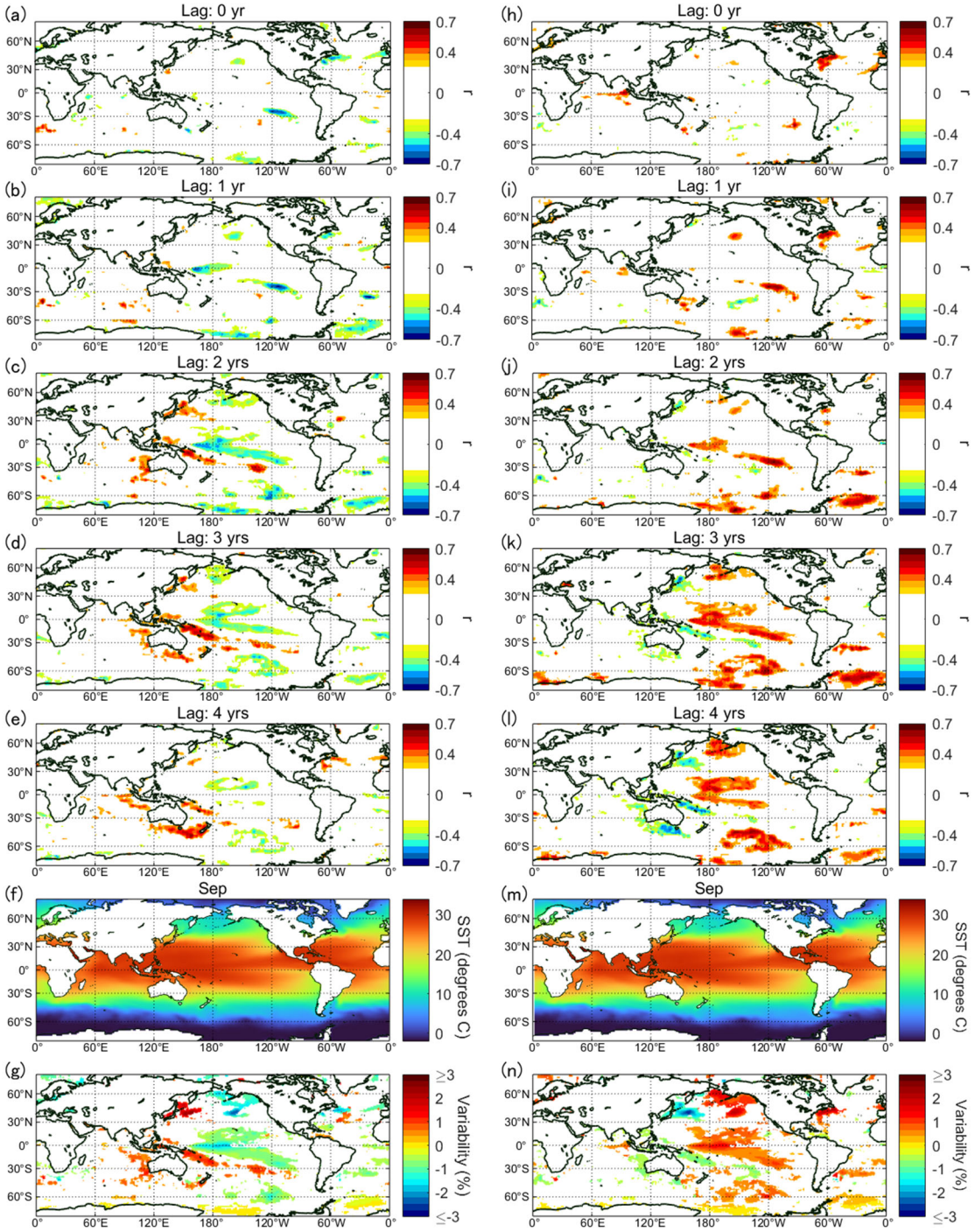

Figure S20. Same as Fig. S13 but for September.

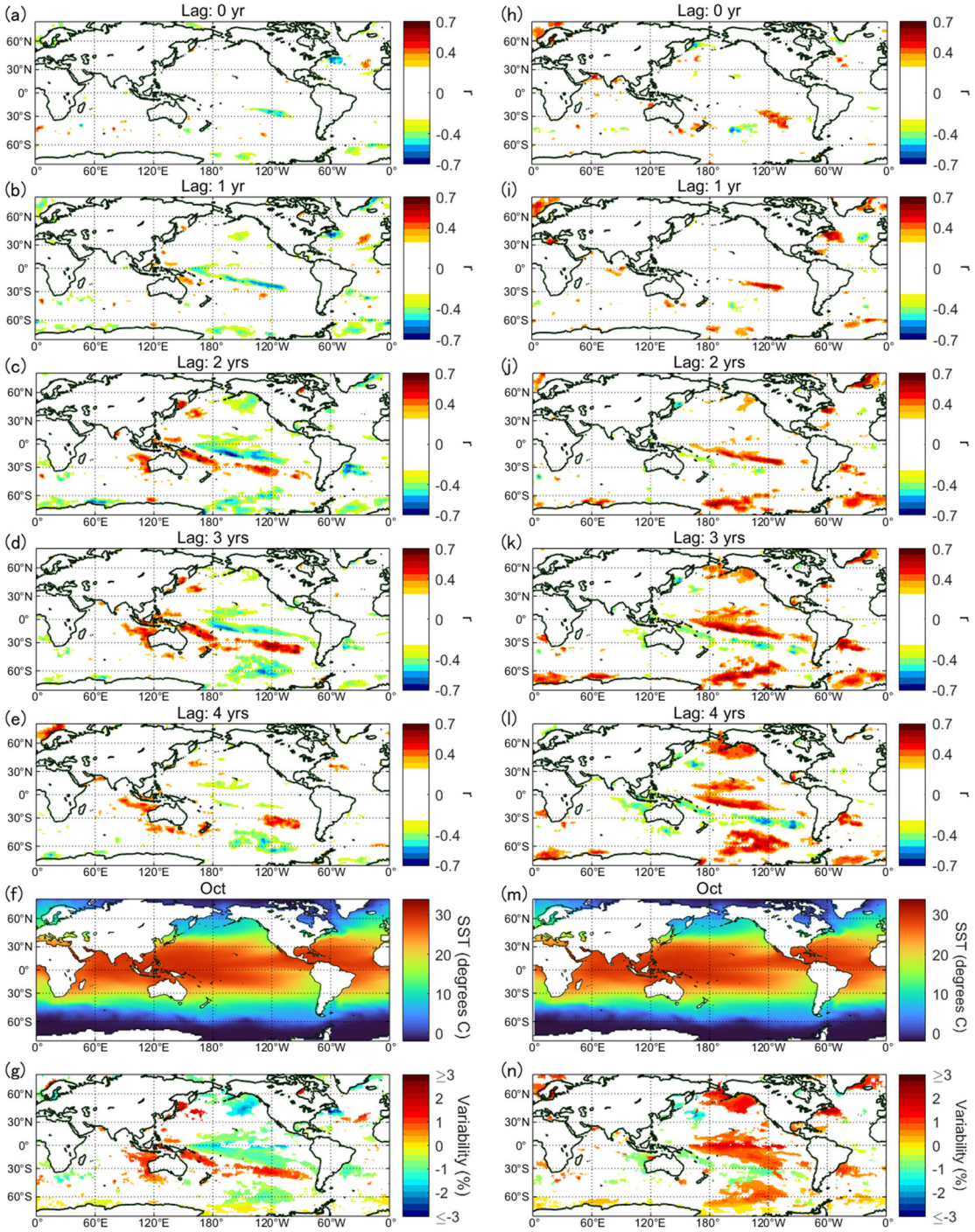

Figure S21. Same as Fig. S13 but for October.

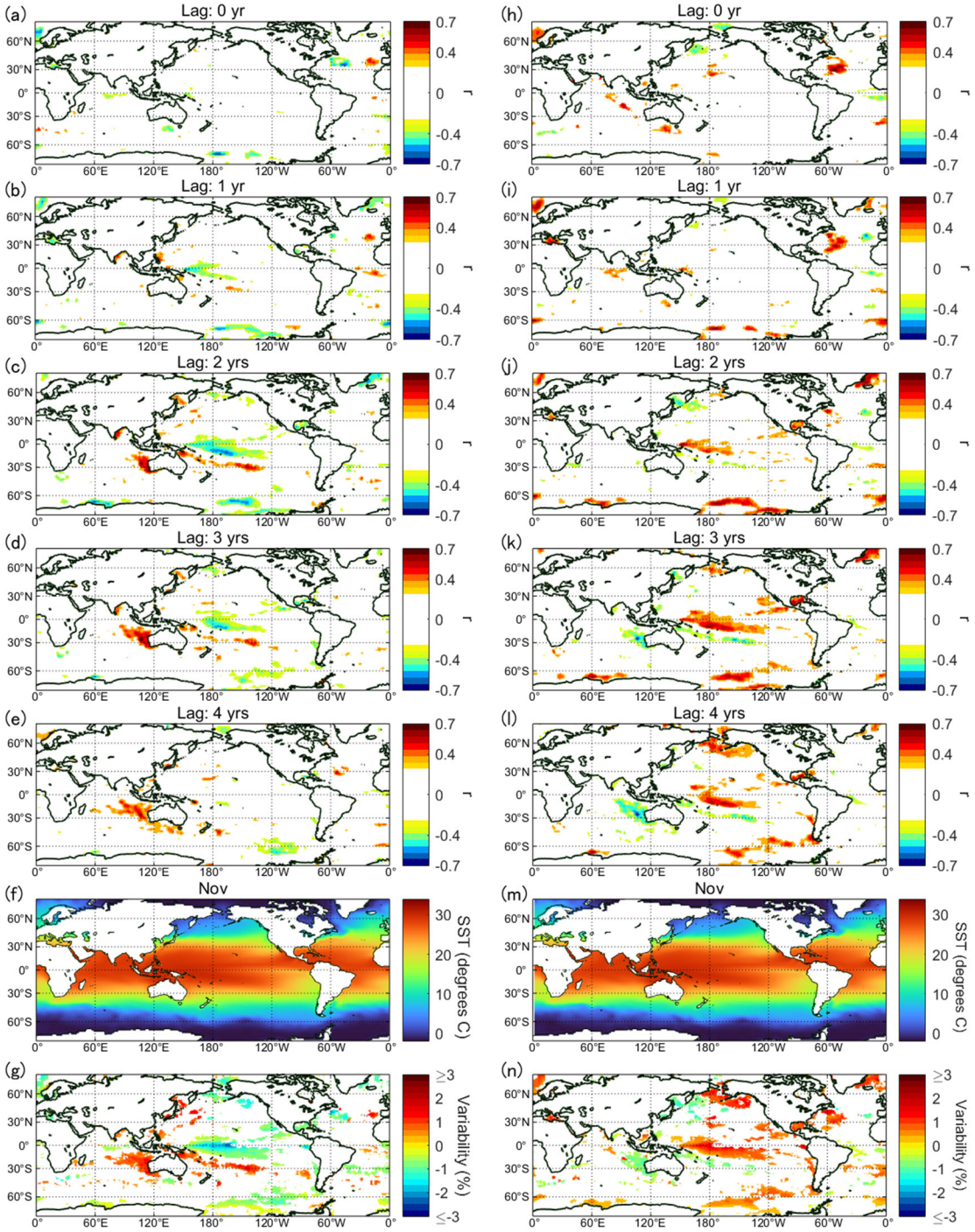

Figure S22. Same as Fig. S13 but for November.

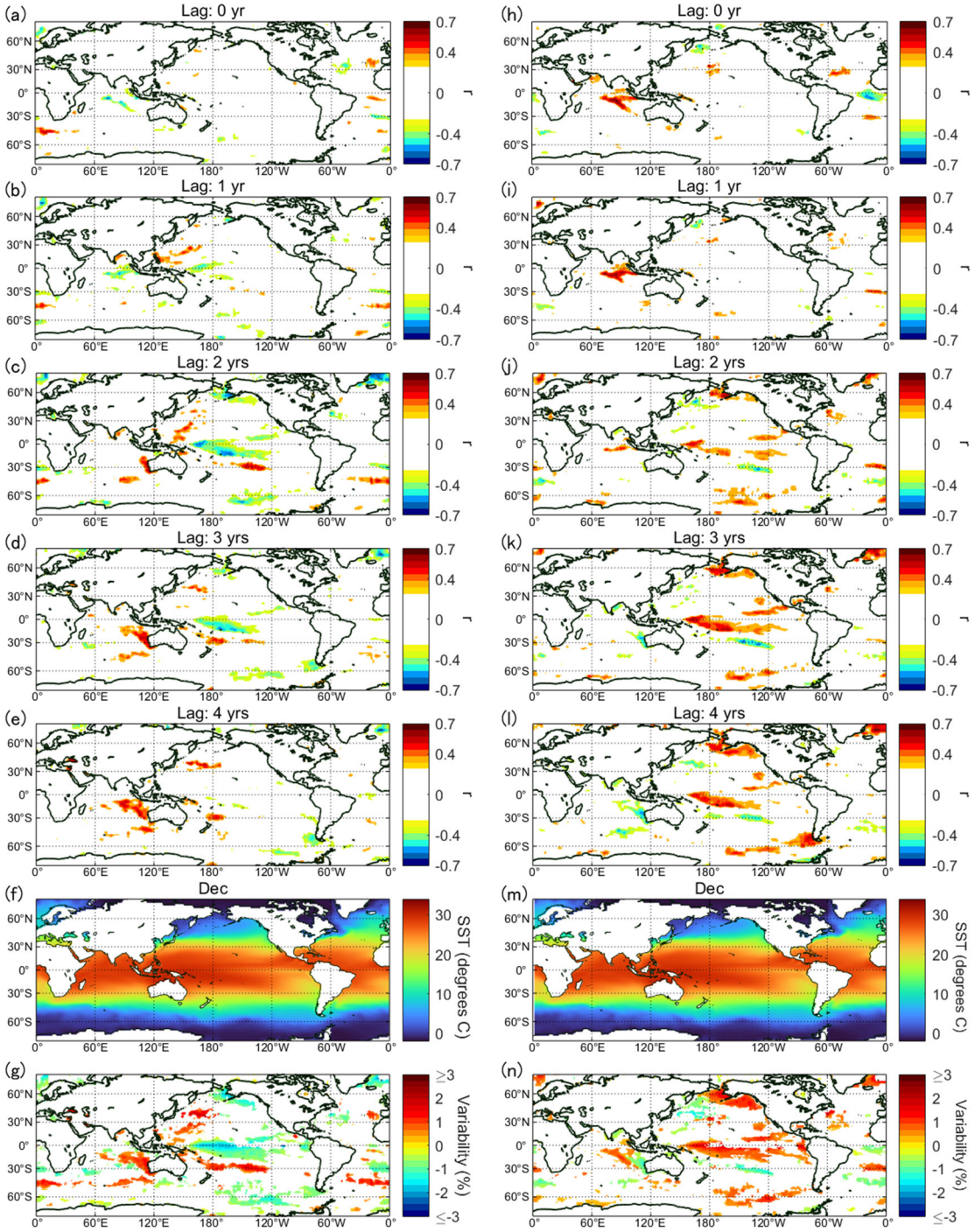

Figure S23. Same as Fig. S13 but for December.

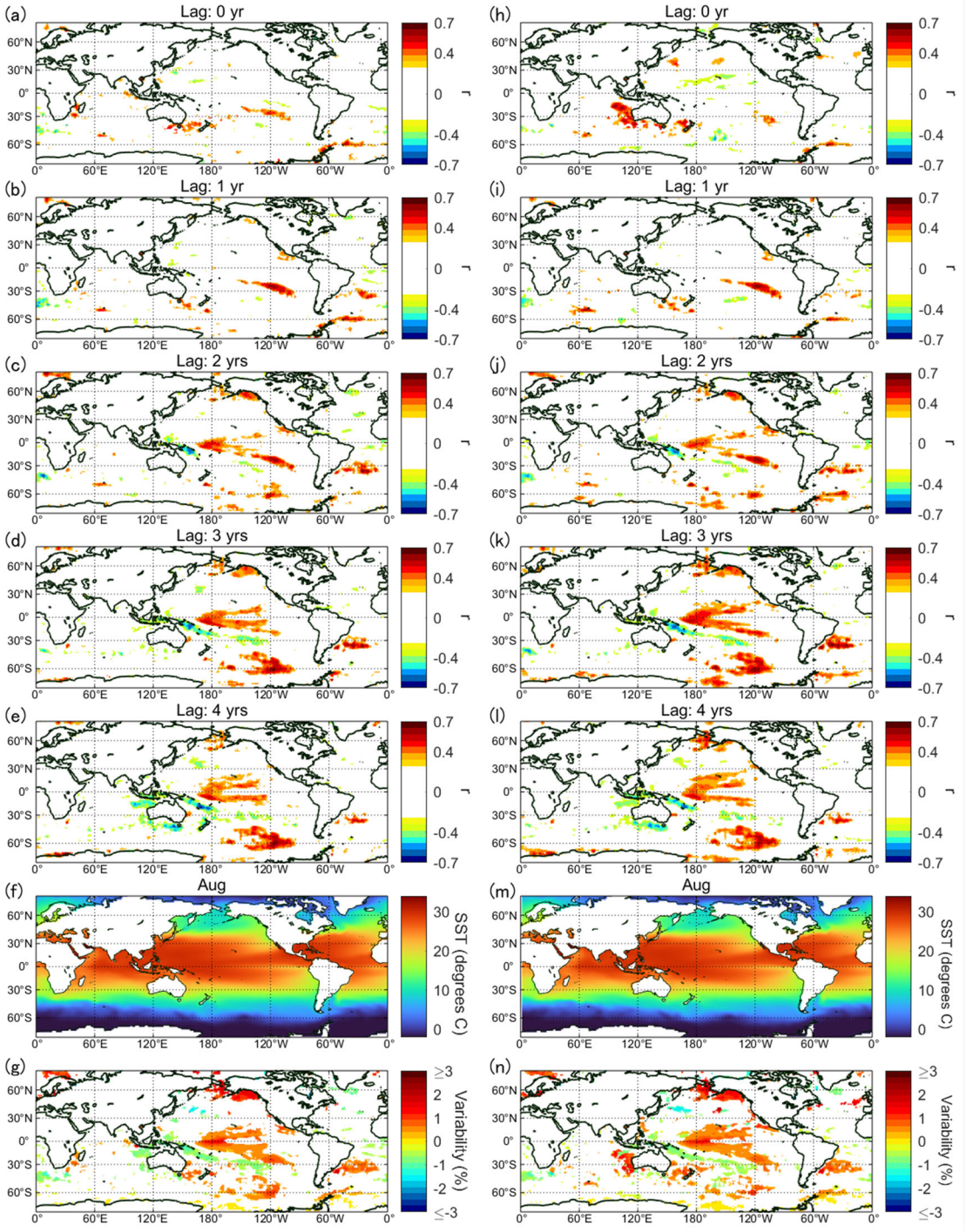

Figure S24. Comparison between SST and SUV/TSI. (a-e) Correlation coefficient r ($p \leq 0.05$) between SUV and SST in August for a lag of 0–4 years, respectively. (f) Monthly mean SST for August. (g) Maximal variability of SST over the SUV cycles. (h-n) Same as (a-g) but for TSI.

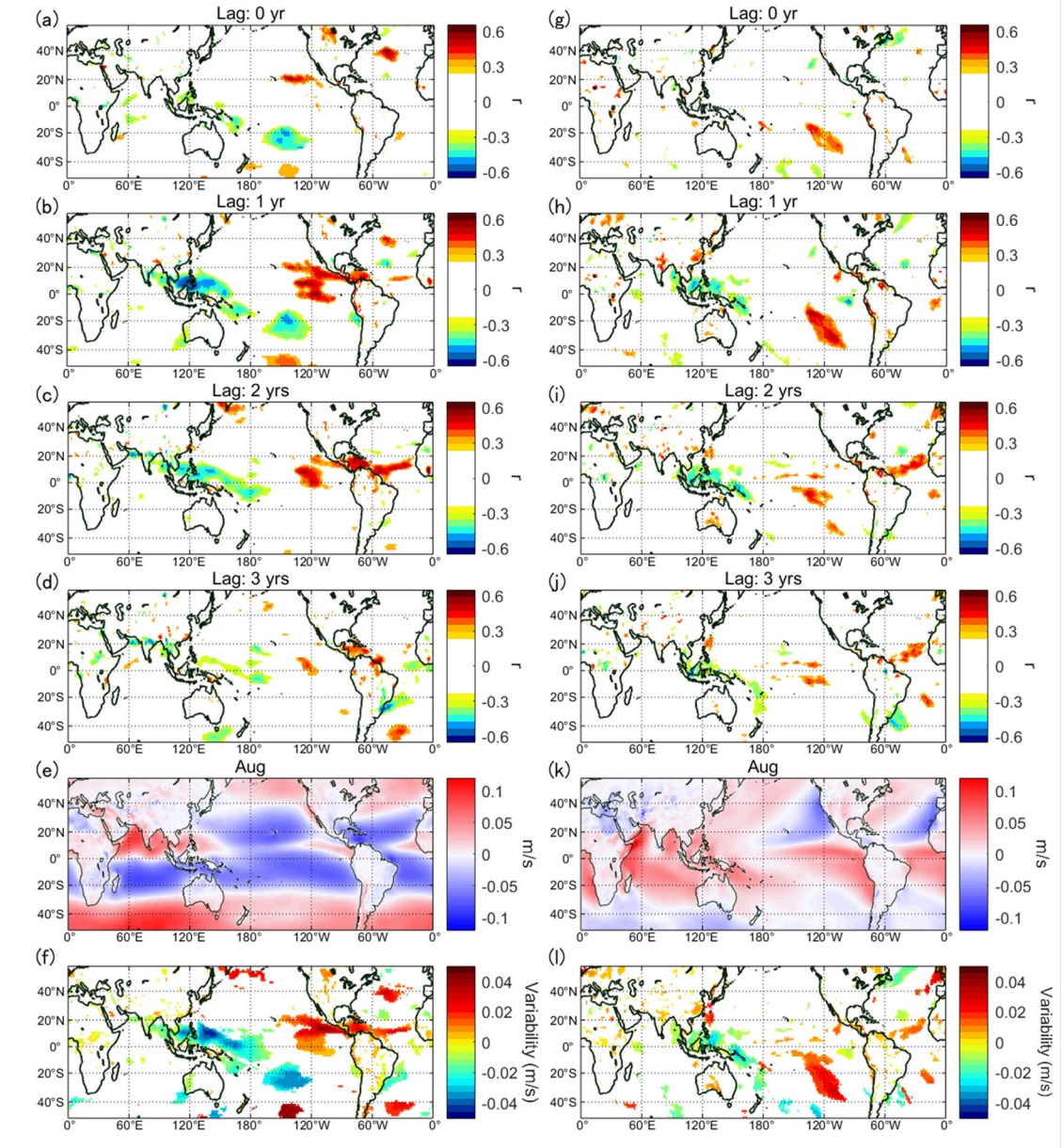

Figure S25. Comparison between the JRA-55 zonal/meridional wind velocity and GCR variation. (a-d) Correlation coefficient r ($p \leq 0.05$) between the zonal wind velocity and GCRs in August for a lag of 0–3 years, respectively. (e) Monthly mean velocity for August. (f) Maximal variability of zonal wind velocity over the GCR cycles. (g-l) Same as (a-f) but for the meridional wind velocity.

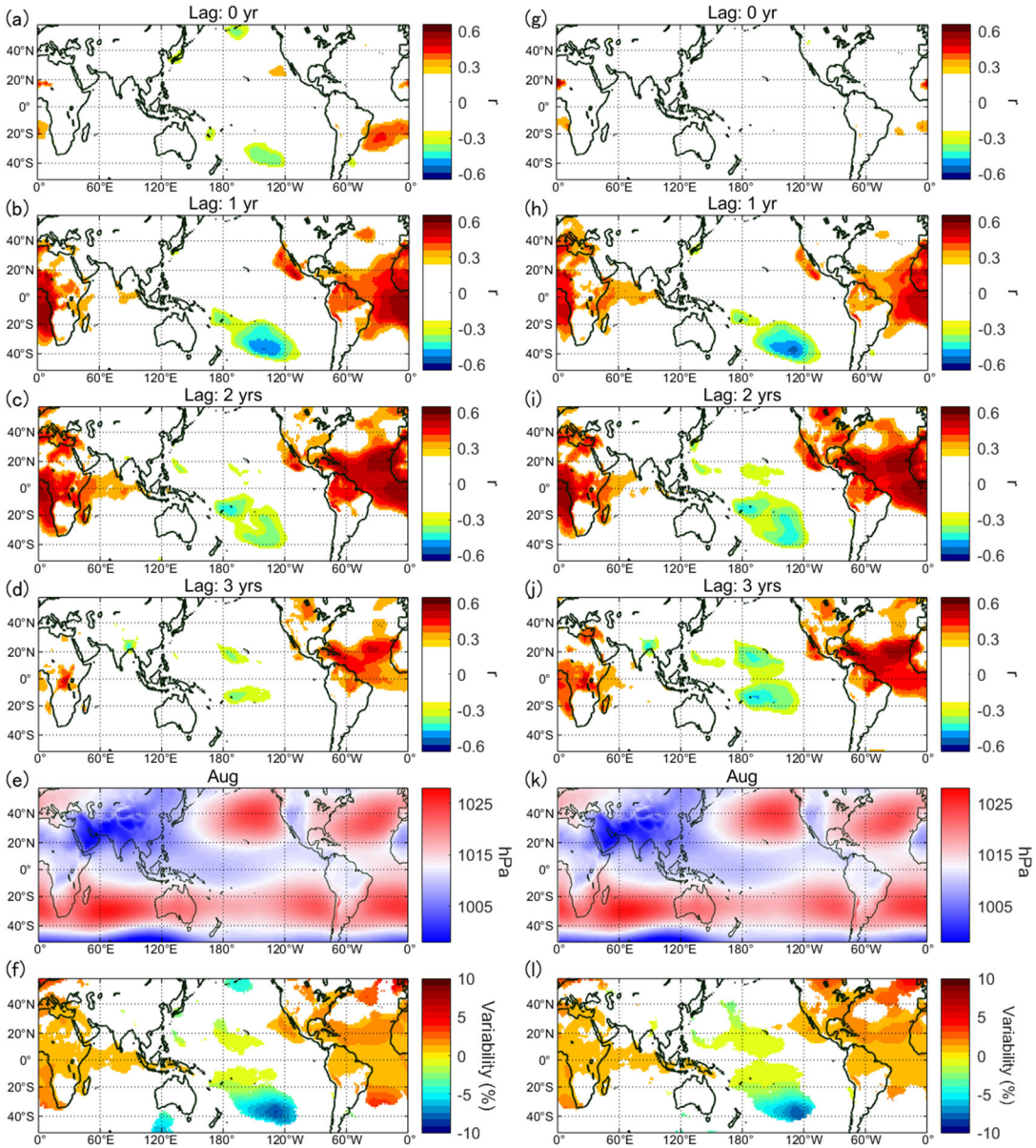

Figure S26. Comparison between the JRA-55 pressure reduced to the mean sea level and the SUV/TSI variations. (a-d) Correlation coefficient r ($p \leq 0.05$) between the pressure and SUV in August for a lag of 0–3 years, respectively. (e) Monthly mean pressure reduced to the mean sea level for August. (f) Maximal variability of pressure over the SUV cycles. (g-l) Same as (a-f) but for TSI.

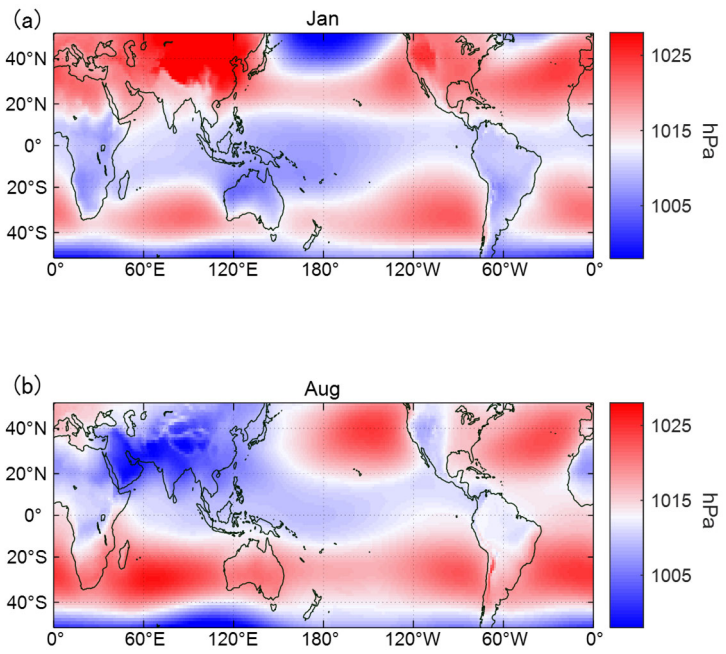

Figure S27. JRA-55 pressure reduced to the mean sea level averaged for 1979–2021 for (a) January and (b) August.

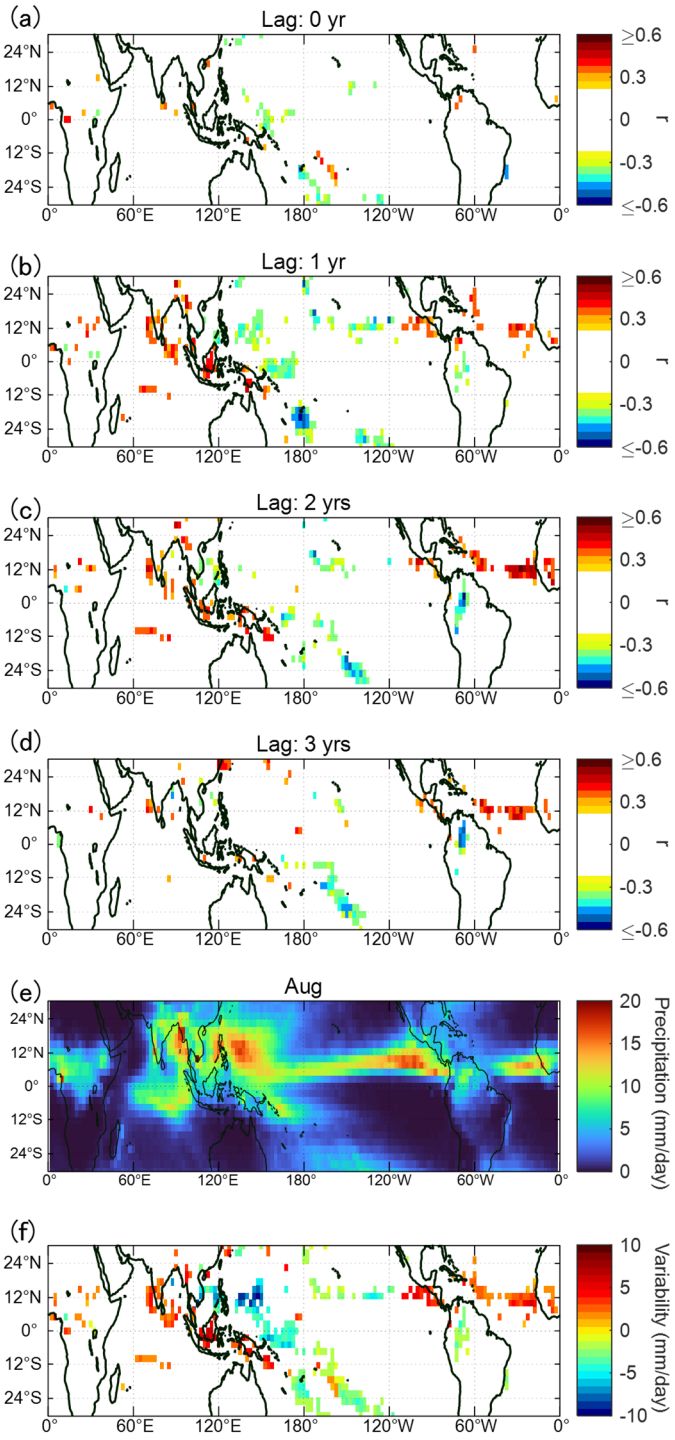

Figure S28. Comparison between the CMAP precipitation data and GCR variation. (a-d) Correlation coefficient r ($p \leq 0.05$) between the precipitation and GCRs in August for a lag of 0–3 years, respectively. (e) Monthly mean precipitation for August. (f) Maximal variability of precipitation over the GCR cycles.

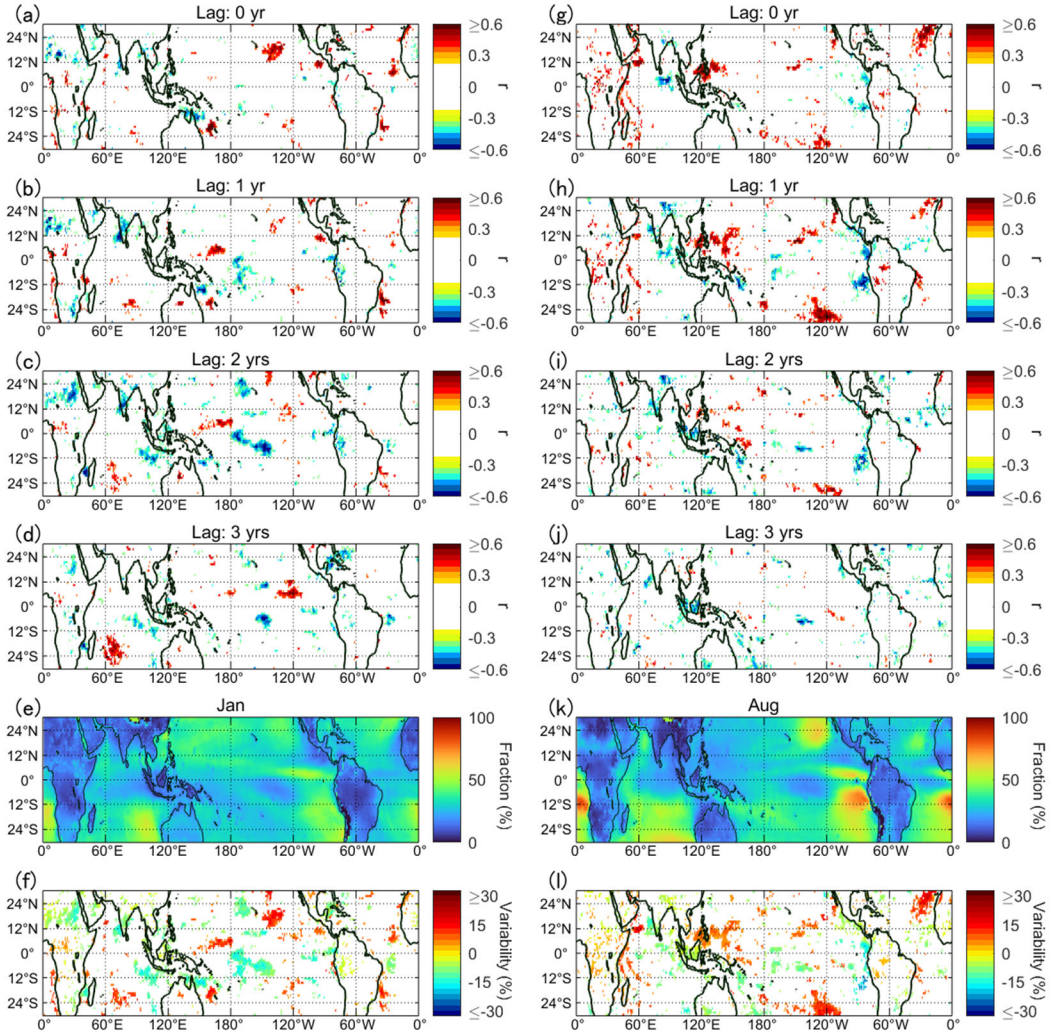

Figure S29. (a-d) Correlation coefficient r ($p \leq 0.05$) between GCRs and the low-altitude cloud fraction in January by ISCCP for a time lag of 0–3 years, respectively. (e) Monthly mean fraction of the low-altitude clouds in January. (f) Maximal variability of the low-altitude cloud fraction over the GCR cycles. (g-l) Same as (a-f) but for August.